# Characteristics of Atmospheric Elemental Carbon(Char and Soot) in Ultrafine and Fine Particles in a Roadside Environment, Japan

**ARTICLE** *in* AEROSOL AND AIR QUALITY RESEARCH · JANUARY 2011

Impact Factor: 2.09



**4 AUTHORS**, INCLUDING:

Kyung Hwan Kim
Korea Institute of Science and Technology
**26** PUBLICATIONS **71** CITATIONS
SEE PROFILE

Kazuhiko Sekiguchi
Saitama University
**60** PUBLICATIONS **425** CITATIONS
SEE PROFILE

*Aerosol and Air Quality Research,* 11: 1–12, 2011

ISSN: 1680-8584 print / 2071-1409 online
doi: 10.4209/aaqr.2010.07.0061

# Characteristics of Atmospheric Elemental Carbon (Char and Soot) in Ultrafine and Fine Particles in a Roadside Environment, Japan

**Kyung Hwan Kim[1], Kazuhiko Sekiguchi[1,2*], Shinji Kudo[1], Kazuhiko Sakamoto[1,2]**

[1] *Graduate School of Science and Engineering, Saitama University, 255 Shimo-Okubo, Sakura, Saitama 338-8570, Japan*
[2] *Institute for Environmental Science and Technology, Saitama University, 255 Shimo-Okubo, Sakura, Saitama 338-8570, Japan*

## ABSTRACT

Atmospheric carbonaceous components, particularly char and soot in ultrafine particles (UFPs; $D$p < 0.1 μm) and fine particles (FPs; $D$p < 2.5 μm), were measured four times during one year in Saitama City, Japan, to observe the concentrations of elemental carbon (EC) and the relationship between the EC concentrations in UFPs and FPs, and to examine the possible emission sources of char and soot that constitute UFPs and FPs in a roadside environment. It was found that EC accounts for 33–37% of total carbon (TC) in FPs, whereas EC accounts for 12–20% of TC in UFPs. Both char-EC and soot-EC account for similar proportions of the total EC concentration in UFPs, while soot-EC accounts for only a small amount of the total EC in FPs. Positive and negative correlations between OC and soot-EC were observed for UFPs and FPs, respectively. The observed positive correlation in the case of UFPs possibly reflects the compactness (high density) of UFPs coated with condensed material, such as unburned fuel or lubricating oil emitted by motor vehicles, whereas the negative correlation in the case of FPs possibly indicates that whether or not the spaces between primary soot particles in FPs can be filled depends on the engine load of diesel vehicles operated near the sampling site. The positive and negative correlations were stronger for UFPs ($r^2$ = 0.69, $n$ = 29, $p$ < 0.001) and FPs ($r^2$ = –0.62, $n$ = 29, $p$ < 0.001) when the data collected at wind speeds greater than 2.5 m/s were excluded. The different morphological characteristics of the particles observed by transmission electron microscopy also support the observed correlations between OC and soot-EC. The possible emission of char or char-like particles from motor vehicles was shown and discussed in this study.

***Keywords***: Black carbon (BC); Ultrafine particles; Char-EC; Soot-EC; Diesel exhausts.

## INTRODUCTION

Black carbon (BC), also referred to as elemental carbon (EC) or light-absorbing carbon (LAC), is one of the key components of atmospheric aerosols that contribute to positive radiative forcing (Ramanathan *et al*., 2001). Recently, atmospheric BC has received considerable attention because of its significant influence on climate change as well as its adverse effects on human health. Atmospheric BC is the dominant anthropogenic absorber of incident solar radiation in the atmosphere (Haywood and Ramaswamy, 1998; Jacobson, 2004a; Ramanathan and Carmichael, 2008). BC also absorbs thermal infrared radiation from the ground (Jacobson, 2004a; Ramanathan *et al*., 2007b) and within clouds (Jacobson, 2006). Furthermore, BC directly heats surfaces on which it is deposited. In the case of snow and ice, this leads to additional melting. Moreover, BC changes the albedo (surface reflectivity) of ice and snow leading to additional warming of the surface and melting (Hansen and Nazarenko, 2004). BC may also influence climate indirectly on a regional scale by altering the monsoon circulation and hydrological cycle (Menon *et al*., 2002; Park *et al*., 2010).

As an absorber of solar radiation, BC is a million times stronger than $CO_2$, but the residence time of BC much shorter than that of $CO_2$. Thus, 20–45% of net global warming potential can be eliminated within 3–5 years by reducing BC with organic matter (OM); the same net global warming potential can also be eliminated by reducing the same amount of $CO_2$, but this would be effective after 50–200 years (Jacobson, 2002, 2004). Globally, the annual emissions of $CO_2$ and BC are 26,939 Tg C and 7.00 Tg C, respectively (Chameides and Bergin, 2002). BC emissions result from the incomplete combustion of carbonaceous fuels, for example: diesel engines for transportation and industrial use; residential combustion of solid fuels such as coal or wood; outdoor burning of biomass; and industrial processes (Mayol-Bracero *et al*., 2002; Bond, 2007). An estimated two-third of BC emissions from energy-related combustion in 2000 was from fossil fuel combustion (Bond

* Corresponding author. Tel./Fax: +81-48-858-9542
*E-mail address:* kseki@mail.saitama-u.ac.jp

*et al*., 2007; Junker and Liousse, 2008) with diesel combustion increasing globally since the mid-1980s (Bond *et al*., 2007).

BC is a generic term that encompasses a continuum of carbon- and aromatic-rich organic compounds that constitute products generated through the combustion of biomass and fossil fuels (Masiello, 2004). Compounds formed in the solid state, such as char/charcoal (the product of incomplete combustion of plant materials) and coal (the product of the metamorphosis of peat deposits), retain some of the original properties of their source materials. Soot, on the other hand, is formed through the high-temperature condensation of hot gases emanating from solid and liquid fuels during combustion; soot retains very few of the physical and chemical properties of its source materials (Veilleux *et al*., 2009). Char tends to absorb UV light while soot tends to strongly absorb infrared light with little spectral dependence (Han *et al*., 2010); thus, the measurement of soot and char concentrations along with possible emission sources would provide useful information for atmospheric aerosol modeling of climate change as well as for emission reduction efforts of light absorbing aerosols.

The Interagency Monitoring of Protected Visual Environment (IMPROVE) protocol with the thermal optical reflectance (TOR) method (Chow *et al*., 1993) can be used to differentiate between char-EC and soot-EC according to its stepwise thermal evolutional oxidation of different carbon fractions under different temperature and atmosphere conditions (Han *et al*., 2007, 2009, 2010). Char-EC and soot-EC are operationally defined as EC1 minus pyrolyzed organic carbon (POC) and EC2 plus EC3 (EC1, EC2, and EC3 correspond to carbon fractions evolved at 550, 700, and 800°C in a 98% He/2% $O_2$ atmosphere, respectively (Han *et al*., 2010). Han *et al*. have reported that char-EC is emitted largely from biomass and coal combustion while soot-EC is emitted largely from motor vehicle emissions and forest fires (2009, 2010).

In order to reduce BC emission from fossil fuel and biomass burning, it is crucial to identify the emission sources. Source identification can potentially be achieved through the interpretation of atmospheric BC particle measurements. The measurement of atmospheric BC, especially fine particles (FPs, $D$p < 2.5 μm), is crucial for source identification because FPs are the primary cause of climatic problems due to their size, which results in longer residence times and long-range transport of the particles. Furthermore, measurement of BC in ultrafine particles (UFPs, $D$p < 0.1 μm) is also important for source identification because the leading removal mechanism of UFPs is agglomeration to form FPs. Thus, measuring BC in UFPs and FPs is expected to be useful to determine the sources of particles as well as to understand further particle formation and growth in the atmosphere.

However, the chemical composition of UFPs and FPs is not well understood and few studies have been conducted on atmospheric char and soot particles, and on the seasonal variation of the characteristics and sources of these particles. Furthermore, studies on atmospheric char and soot concentrations, particularly UFP concentrations, are scarce; thus, determining the concentration levels of char and soot in atmospheric UFPs and FPs would be valuable to examine the possible emission sources and the constituents of particles of these two sizes.

Therefore, the objectives of this study are 1) to measure the concentration of BC in UFPs and FPs in a roadside environment, 2) to determine the seasonal variation of BC in UFPs and FPs, 3) to observe the relationship between the BC concentrations of UFPs and FPs, and 4) to identify the sources of char and soot in UFPs and FPs in a roadside environment.

## EXPERIMENTAL

### *Sampling Site and Sample Collection*

Saitama City, Japan, is located on the Kanto Plain at 35.867°N, 139.65°E to the Northwest of the Tokyo Metropolis (Fig. 1) and the city is around 20 km away from central Tokyo Metropolis. Therefore, the city can be affected by pollutants not only from Tokyo and other industrial areas near the ocean during summer due to summer East Asian monsoon (Seasonal reversing wind from Southeast to Northwest), but also from China or the northern Asian continent during winter, as a result of winter East Asian monsoon (Hagino *et al*., 2007). Field sampling was carried out during summer (July to August 2009), fall (October 2009), winter (January 2010), and spring (April 2010) for 14 days in each season. The meteorological conditions during the sampling periods were typical for Saitama City during the corresponding seasons. The sampling site was located on a roadside at the front gate of the Saitama University campus, which is surrounded by residential areas and located near the intersection of two roads.

A Cyclone $PM_{2.5}$ (University research glassware, Co Inc., NC, USA) operated at 16.7 L/min and an inertial fibrous filter (INF) sampler (Kanomax Japan, Inc., Osaka, Japan) operated at 40 L/min were used for the collection of FPs and UFPs, respectively. The INF sampler consists of four impaction stages that remove particles with diameters of 10, 2.5, 1.0, and 0.5 μm, respectively. The system also has one inertial filtration stage composed of unwoven stainless steel fibers which removes particles larger than 0.1 μm after the four impaction stages; then, UFPs are collected uniformly onto a 47-mm quartz filter (Otani *et al*., 2007; Eryu *et al*., 2009; Furuuchi *et al*., 2010a, b).

The sampling duration was 23.5 h, which corresponds to a total sampling volume of 56.5 and 23.5 $m^3$ for the collection of UFPs and FPs, respectively. Quartz fiber (2500 QAT-UP, Pallflex, CT, USA) filters were pre-baked at 900°C for 3 h to remove possible contamination. Pre-baked filter blanks were measured prior to sampling, and eight field blanks were measured during each field sampling campaign. The field blanks were placed in a same container with sample filters, transported to the field and treated as a sample including contact with the sampling devices and exposure to the sampling site condition, storage, preservation, and all analytical procedures. Field

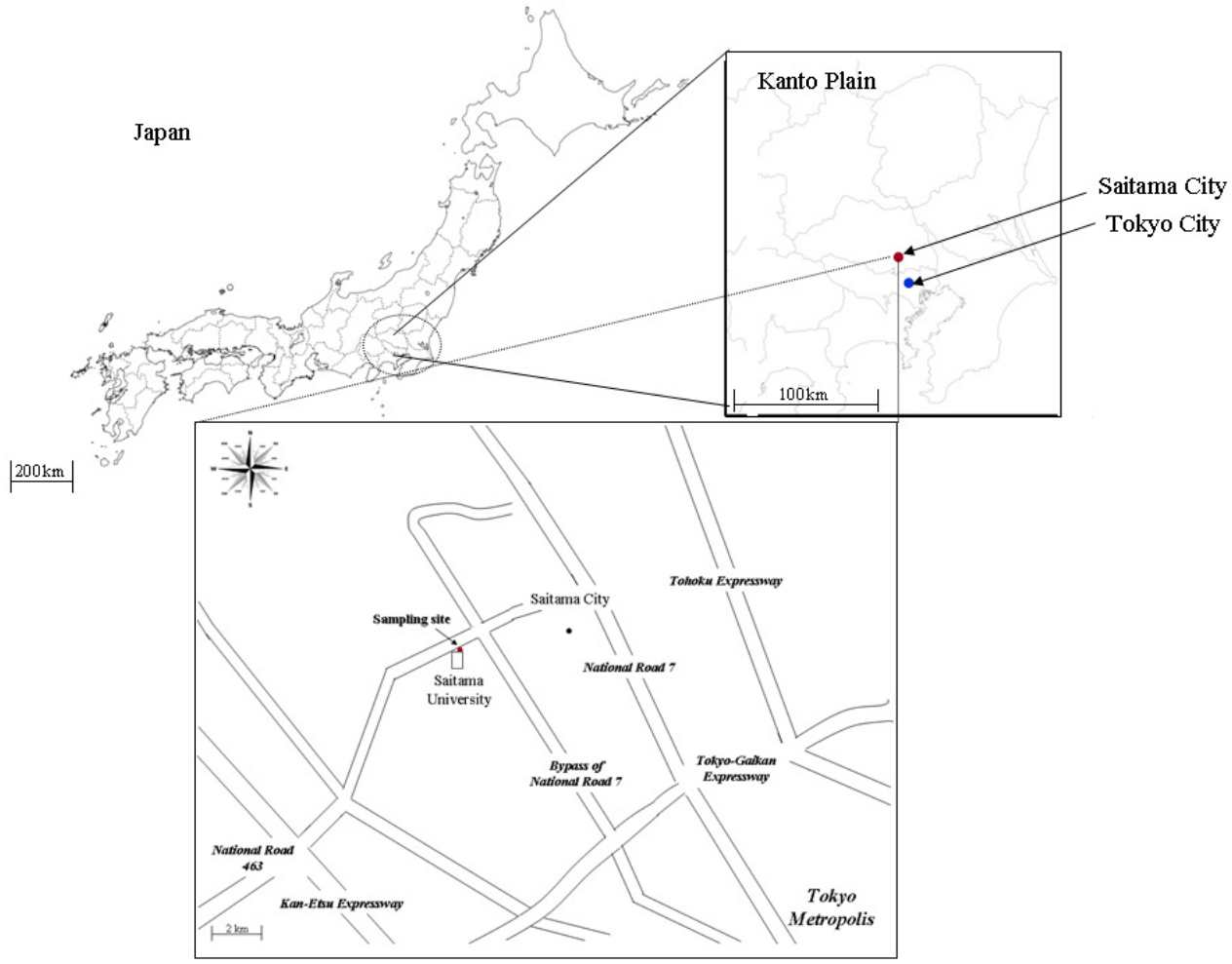


**Fig. 1.** Sampling location.

blanks with unusually high or low values compared to the rest of the blanks were excluded based on the measured average field blank with standard deviations. The blank subtraction was performed based on the field blanks for the samples collected each season.

### *Analysis of OC, EC, and Morphology of Collected Particles*

Carbon analyses were carried out on a Desert Research Institute (DRI) Model 2001 Carbon Analyzer (Atmoslytic Inc., Calabasas, CA) following the IMPROVE_TOR method. The particle collected sample was punched for specific size (0.501 $cm^2$) then placed onto the sample load position of the analyzer. Inside of the analyzer during the analysis, the sample was heated to produce four OC fractions (OC1, OC2, OC3, and OC4) at temperatures of 120, 250, 450, and 550°C, respectively, in a non-oxidizing helium atmosphere, as well as three EC fractions (EC1, E2, and E3) at 550, 700, and 800°C, respectively, in an oxidizing atmosphere of 2% $O_2$/98% He. At the same time, POC was produced in the inert atmosphere, which decreased the reflected light to correct for charred OC. More detailed information about the analysis of OC and EC by the IMPROVE_TOR method can be found elsewhere (Chow *et al*., 2001, 2004; Han *et al*., 2007, 2009, 2010). In this study, OC1, OC2, OC3, and OC4 were defined to exclude the POC concentration. The EC fraction was divided into char-EC and soot-EC (Han *et al*., 2007, 2009, 2010). Char-EC is defined as EC1 minus POC, and the soot-EC is defined as the sum of EC2 and EC3. The total OC is defined as the sum of the four OC fractions plus POC, and the total EC is define as the sum of the three EC fractions minus POC.

The morphology of the collected particles was observed by transmission electron microscopy (TEM; FEI Tecnai G2 20; accelerating voltage: 120 kV) because char and soot have different morphological characteristics, and also because soot particles can exhibit different morphological characteristics depending on OC concentration (Park *et al*., 2003). The TEM samples were taken from the particle collected quartz filters and transferred to a TEM substrate using a cleaned needle carefully. Copper 200 mesh grids coated with carbon and silicon monoxide films were used as the TEM substrates.

### *Meteorological and Other Gas Pollutants Data*

A meteorological station (Saitama Institute of Public Health) is located within 0.8 km from the sampling site.

Data on NO, $NO_2$, $NO_x$, oxidants, UV radiation, temperature, relative humidity, wind direction, and wind speed are acquired hourly.

## RESULTS AND DISCUSSION

### *Concentration of Carbonaceous Components*

Table 1 shows the average concentrations of carbonaceous species in FPs and UFPs. Generally, the measured amount of carbonaceous components tended to increase from summer to winter. The higher concentrations of the fall and winter samples indicate that the increased concentrations of pollutants were possibly related to increased energy (fuel) consumption and illegal biomass burning around the sampling site. Also, atmospheric aerosols could be trapped by poor ventilation during the fall and winter, considering the relatively stable atmospheric conditions (low mixing height). Furthermore, it is also possible that the transport of pollutants from northern Chinese cities and cities to the north of Saitama City contributed to the air quality at the sampling site in fall and winter, owing to the Asian winter monsoon (Hagino *et al*., 2007). Average OC and EC concentrations in FPs during the four seasons were 5.50 ± 0.99 and 2.88 ± 0.58 μg/m$^3$ respectively with 2.03 ± 0.9 OC/EC ratio. One study in Osaka, Japan (Funasak *et al*., 1998) which was carried out at roadside for $PM_{2.0}$ using a cascade impactor showed 5.2 and 3.4 μg/m$^3$ for the average OC and EC respectively with 1.53 OC/EC ratio. Another study carried out in Hong Kong, China (Ho *et al*., 2004) carried out at roadside for $PM_{2.5}$ collection using a mini volume sampler showed 12.6 ± 5.4 and 6.4 ± 2.8 μg/m$^3$ for the average OC and EC respectively with 2.0 ± 0.4 OC/EC ratio.

Interestingly, char-EC dominated the total EC in FPs for all samples, while char-EC accounted for only 40 to 50% of the total EC in UFPs, indicating that the contribution of soot-EC was significant in UFPs. Char-EC in FPs and UFPs tended to increase from summer to winter reflecting that increased energy consumption related to heating systems and biomass burning may have contributed to the char-EC concentrations. In contrast, soot-EC in FPs reached the highest concentration in summer, whereas soot-EC in UFPs tended to increase from summer to winter. The increased summer soot-EC in FPs was possibly transported by summer monsoon from Tokyo or other southern cities near the ocean.

### *OC and EC Components*

*Seasonal Variation of OC and EC Fractions*

The seasonal variation of OC and EC fractions is shown in Fig. 2(a) and (b). The concentrations of these components in FPs were approximately 10 times higher than those observed in UFPs. As the main carbon fractions, EC1 and OC2, respectively, accounted for 38% and 20% of TC in FPs, while OC2 and OC3, respectively, accounted for 42% and 30% of TC in UFPs. EC3 was not observed in the FP and UFP samples in this study.

*Correlation between OC and EC during Different Seasons*

The correlation between OC (x-axis) and EC (y-axis) in FPs and UFPs is shown in Fig. 3(a) and (b), respectively; these plots show the relative contribution of OC and EC to the composition of the particles during the sampling period in each season. Generally, slopes ranged from 0.53–0.64 in FPs except for the fall samples (0.26). Biomass burning, which is frequently carried out in fall, or regionally transported FPs may have led to the different correlation between OC and EC for the fall samples.

In the case of UFPs, the slopes ranged from 0.18 to 0.24 and tended to decrease from summer to winter, indicating that the OC/EC ratio in UFPs tended to decrease from summer (average: 18.06 ± 6.17) to winter (average: 5.95 ± 0.94). As shown in Fig. 3, a different correlation between OC and EC in FPs for fall samples was observed, whereas this was not observed in the case of UFPs. Therefore, the carbonaceous components in UFPs may have been influenced by freshly emitted particles around the sampling site, rather than regionally transported particles or biomass burning.

*Correlations of Char-EC with OC, EC, and Soot-EC*

The observed correlations of char-EC with OC, EC, and soot-EC in FPs and UFPs are plotted all together to show an overview of the relationships. As shown in Fig. 4(a), char-EC in FPs had a strong positive correlation with OC and EC, while char-EC in FPs had a moderate negative correlation with soot-EC. On the other hand, char-EC in UFPs had only positive correlations with OC, EC, and soot-EC.

Char-EC had the strongest correlation with OC and EC in FPs, indicating that char-EC dominated the total EC and had a close relationship with OC, as shown in Fig. 4(a). This finding is consistent with the studies by Han *et al.* (2009, 2010). Char-EC showed a moderate negative correlation with soot-EC, indicating that soot-EC concentrations decreased with the char-EC concentrations in FPs. On the other hand, char-EC in UFPs showed a positive correlation with OC, EC, and soot-EC in UFPs (Fig. 4(b)), which is notably different from the observed correlation for FPs, indicating that the relationship between char-EC and soot-EC in UFPs is different from that observed in FPs.

The formation of soot-EC can be considered to decrease as the formation of OC and char-EC increases from the same sources for FPs because the soot-EC in FPs showed negative correlations with OC and char-EC. On the other hand, the formation of soot-EC proportionally increased as the formation of OC and char-EC increased from the same sources for UFPs because the soot-EC in UFPs showed positive correlations with OC and char-EC. In order to find the relationship between OC, char-EC, and soot-EC in UFPs and FPs, further data analysis was carried out, taking into account the characteristics of particles emitted from motor vehicles.

*Different Correlations of Soot-EC with OC in FPs and UFPs*

The correlations between soot-EC and OC in FPs and UFPs were further analyzed for different seasons, because soot-EC in FPs was found to have a stronger negative

**Table 1.** Average concentration of carbonaceous components.

| Chemical species | FPs | | | | UFPs | | | |
|---|---|---|---|---|---|---|---|---|
| | 2009 Summer | 2009 Fall | 2010 Winter | 2010 Spring | 2009 Summer | 2009 Fall | 2010 Winter | 2010 Spring |
| OC (μg/m$^3$) | 3.32 ± 0.52 | 7.61 ± 0.94 | 6.70 ± 1.48 | 4.38 ± 1.02 | 0.87 ± 0.08 | 1.12 ± 0.13 | 1.12 ± 0.14 | 0.84 ± 0.18 |
| EC (μg/m$^3$) | 2.32 ± 0.44 | 3.69 ± 0.38 | 3.38 ± 0.79 | 2.14 ± 0.69 | 0.11 ± 0.07 | 0.19 ± 0.03 | 0.20 ± 0.04 | 0.10 ± 0.04 |
| Char-EC (μg/m$^3$) | 1.85 ± 0.43 | 3.48 ± 0.40 | 3.60 ± 0.84 | 1.88 ± 0.71 | 0.06 ± 0.02 | 0.08 ± 0.01 | 0.10 ± 0.02 | 0.06 ± 0.02 |
| Soot-EC (μg/m$^3$) | 0.47 ± 0.06 | 0.21 ± 0.04 | 0.28 ± 0.06 | 0.26 ± 0.10 | 0.03 ± 0.02 | 0.11 ± 0.02 | 0.10 ± 0.02 | 0.04 ± 0.02 |

± indicates standard deviation of concentrations.
$n$ = 13 for summer FPs, $n$ = 14 for FPs and UFPs collected in other seasons.
Char-EC = EC1 – POC, Soot-EC = EC2+ EC3.

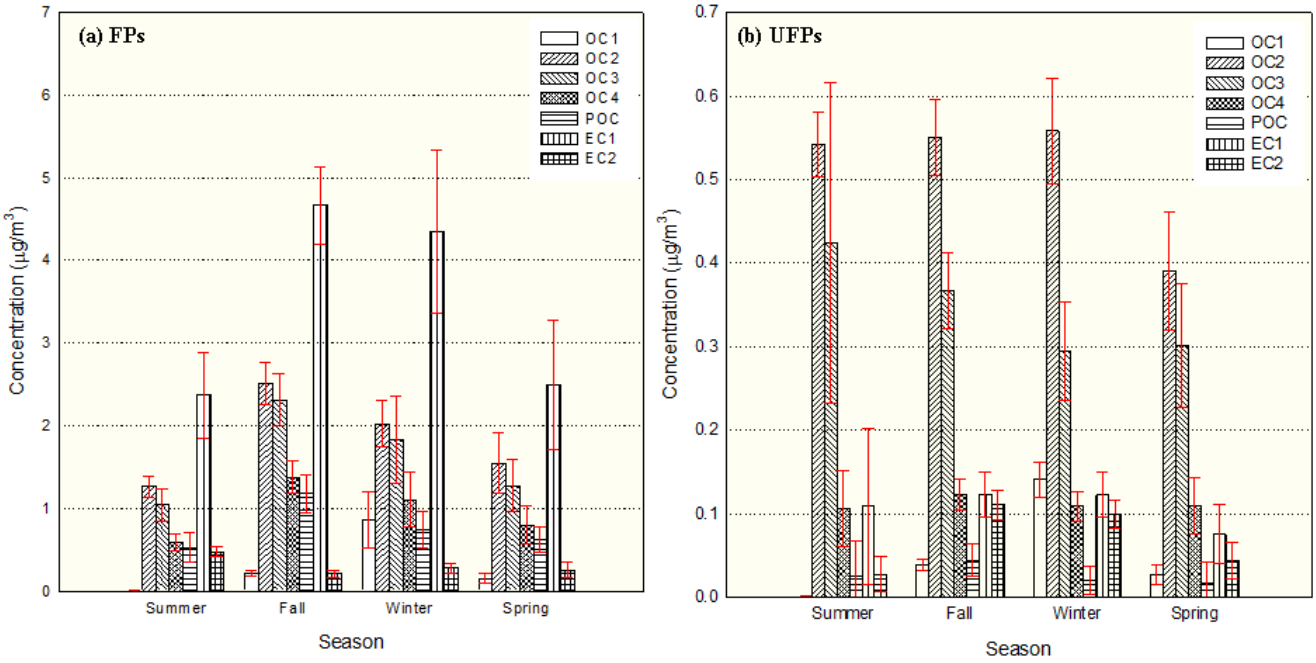


**Fig. 2.** Seasonal variation of OC and EC concentrations in (a) FPs and (b) UFPs.

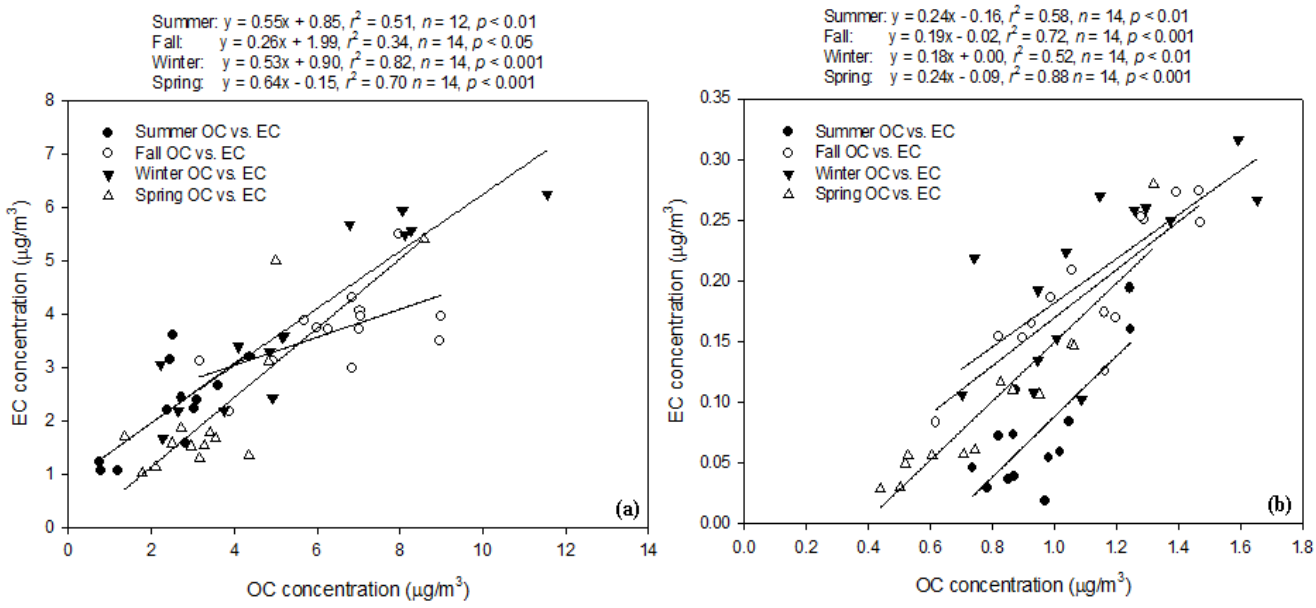


**Fig. 3.** Correlations between OC and EC concentrations in (a) FPs and (b) UFPs.

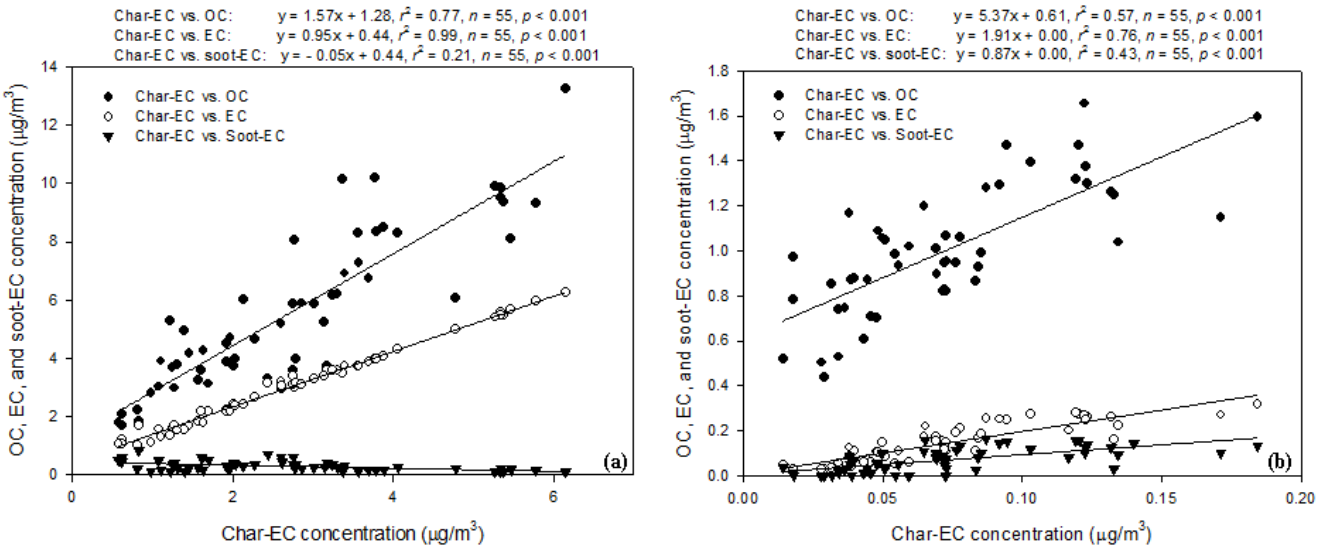


**Fig. 4.** Correlations of char-EC with OC, EC, and soot-EC in (a) FPs and (b) UFPs.

correlation with OC than char-EC, as shown in Fig. 5. Summer samples showed no correlation between soot-EC and OC. Unstable and neutral atmospheric condition with a high mixing height in summer may have led to the insignificant correlation between them. For samples collected in all seasons except summer, soot-EC and OC showed high correlation coefficients, which were negative in FPs and positive in UFPs.

On the basis of this observation, we hypothesized that this tendency might be related to the combustion characteristics of motor vehicles, particularly for diesel vehicles. Because the sampling location was close to the intersection of two roads, it can be thought that the operation of motor vehicles in various drive modes (i.e., deceleration, idling, acceleration, and constant velocity) could significantly influence the particle emissions around the sampling site. To find the different relationship between char-EC, soot-EC, and OC in FPs and UFPs, all data for the four seasons are plotted together in Fig. 6.

The overall correlations of OC with char-EC (Fig. 6(a)) and soot-EC (Fig. 6(b)) in FPs and UFPs show that the concentration of soot-EC in FPs is totally different from that of char-EC. The observed concentration changes of soot-EC against the OC concentration in FPs contradicts the result obtained by Cao *et al.* (2006), who observed a strong positive correlation ($r^2$ = 0.83) between OC and soot-EC (EC2 + EC3) in FPs using a Cyclone $PM_{2.5}$ (5 L/min). However, the sampling sites and the sampling periods differed between the study by Cao *et al.* and the present study. Their sampling site was surrounded by heavily trafficked roads leading to a tunnel, and the sampling was carried out for only one week (from May to June) to observe diurnal variation. In their study, the observed soot-EC concentrations ranged from 5–13 μg/m$^3$

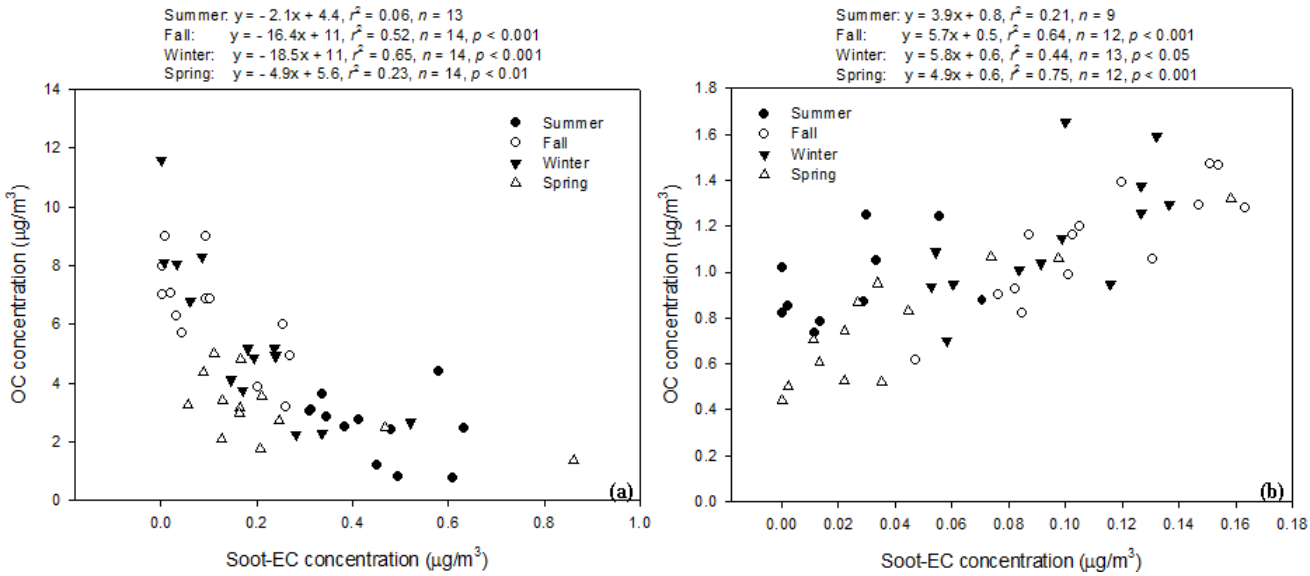


**Fig. 5.** Correlations between soot-EC and OC concentrations in (a) FPs and (b) UFPs.

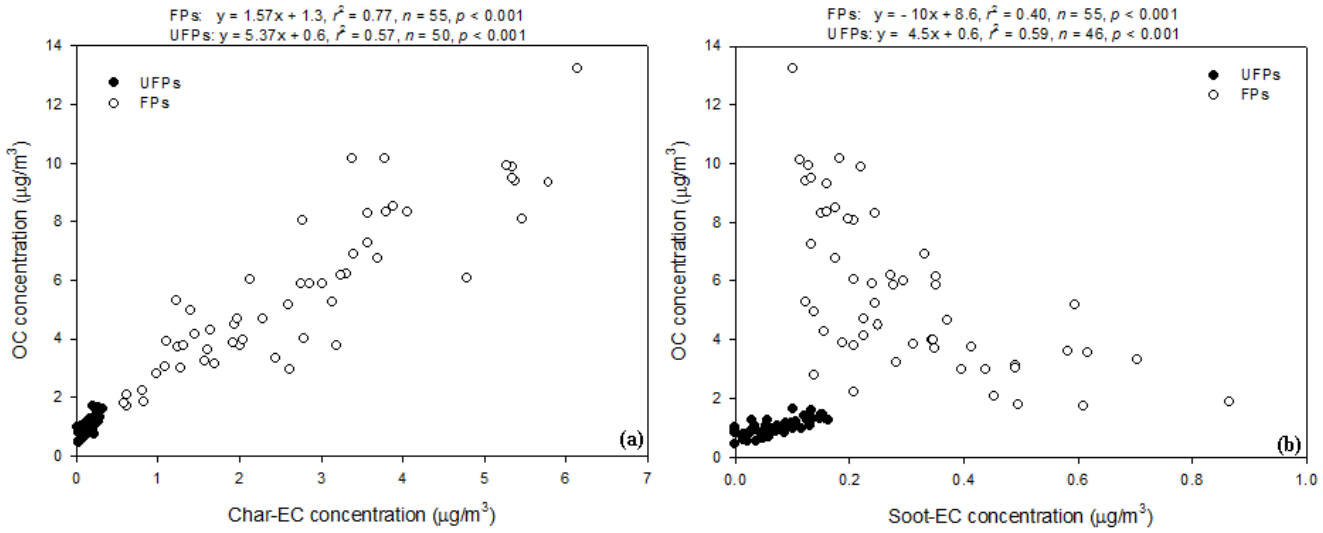


**Fig. 6.** Correlations of OC with (a) char-EC and (b) soot-EC concentrations in FPs and UFPs over the four seasons.

and the TC concentration ranged from 25–40 μg/m$^3$, which was much higher than the values found in the present study. Here, the sampling site was close to an intersection where emissions from motor vehicles operated in different driving modes could be observed. Furthermore, a number of heavy cargo trucks with diesel engines use the roads, which connect three highways (within 5–10 km from the sampling site) leading to Tokyo. This may be the biggest reason for the difference in the observed correlation between OC and soot-EC in FPs.

Soot agglomerates provide a large surface area for adsorption that suppresses nucleation; thus, diesel engines with low soot mass emissions may have high number emissions (Kittelson, 1999). Symonds *et al.* (2007) observed that the diesel soot loading rate changes with driving mode. They found that the soot mass loading rate increases greatly during acceleration and increases slightly during deceleration, indicating that both acceleration and deceleration generate large soot mass emissions to the ambient air. Furthermore, Symonds *et al.* (2007) also found that particle number in accumulation mode increases with acceleration and particle number in nucleation mode increases with deceleration. It has been known that a diesel engine emits high soot mass at high engine load (e.g., acceleration) and low soot mass at low engine load (e.g., driving mode or deceleration) whereas the volatile organic species (e.g., unburned fuel or lubricating oil) is lower at high engine load and much higher at low engine load (Park *et al*., 2003). If a diesel engine emits high soot mass, the number of larger particle would increase via agglomeration and the number of smaller particles would decrease, while the produced volatile organic species would be insufficient to be adsorbed or condensed onto soot particles. On the other hand, if a diesel engine emits low soot mass, the number of larger particle would decrease due to suppression of agglomeration and the number of smaller particles would increase, while much more volatile organic species would be available to be adsorbed or condensed onto soot particles. This could be one reason for the positive and negative correlations between soot-EC and OC in UFPs and FPs, respectively.

There is also strong evidence supporting the negative correlation between soot-EC and OC in FPs and the positive correlation in UFPs. Park *et al.* (2003) studied the effective density and fractal dimension of diesel particles as a function of engine load. They found that the effective density of diesel engine particles (DEPs) changed depending on engine load. Their TEM images showed that DEPs are chain agglomerates consisting of primary particles of between 20 and 40 nm. The smallest particles (50 nm), which had the highest effective density, were found to be the most compact in shape and the 50 nm particles appeared to be coated with condensed material, leading to their compactness. As size increased, the particles became more irregular and agglomerated, consistent with the observed lower effective density. However, Park *et al.* also observed in TEM images that DEPs with a mobility equivalent diameter of 220 nm at low engine load (10% load) appeared more compact than the 220-nm particles produced at a high engine load. They believed that this may have occurred because much more volatile species (e.g., unburned fuel or lubricating oil) are available to adsorb or condense on soot at low engine loads (Kittelson, 1998). The volatile organic fraction decreased with increasing load from 60% at 10% load to about 15% at 75% (Park *et al*., 2003). Thus, the spaces between primary particles were filled, especially for the particles collected at low engine load where higher levels of semivolatile compounds are expected, probably due to the condensation of vapors on those particles. Also, re-entrainment of soot particles from a tailpipe of motor vehicles (Kittelson, 1999) is a possible way to emit larger soot particles with relatively low OC content.

Therefore, the observed positive correlation between OC and soot-EC in UFPs may reflect the compactness of UFPs coated with condensed material such as unburned fuel or lubricating oil. The negative correlation between soot-EC and OC in FPs may also indicate that whether or not the

spaces between primary particles in FPs can be filled depends on the engine load of diesel vehicles around our sampling site. The positive and negative correlations were stronger for UFPs ($r^2$ = 0.69, $n$ = 29, $p$ < 0.001) and FPs ($r^2$ = –0.62, $n$ = 29, $p$ < 0.001) when the data collected at wind speeds greater than 2.5 m/s were excluded. This further confirms the strong influence of motor vehicles around the sampling site. These observations may also reflect the particle formation and growth around roadside environment and the possibility that char-EC could also be emitted by diesel vehicles, considering the negative correlation between char-EC and soot-EC in FPs and the strong positive correlation between OC and $NO_x$. The possibility of char-EC emission by motor vehicles is discussed in Section 3.2.5.

*Possibility of Char Emission by Motor Vehicles*

It has been believed that char is mainly produced from coal and biomass combustions; thus, it has often been used as an indicator for source identification (Han et al., 2009, 2010). In our study, it was found that char-EC concentrations varied from 1.88–3.60 μg/m$^3$ over the four seasons and peaked in winter. Relatively high char-EC concentrations in FP samples collected on a roadside were observed for the seasonal variation study. We attempted to identify the source of char-EC in UFPs and FPs. In fall and winter, the air mass transport from northern Chinese cities as well as from cities to the north of the sampling site and biomass burning during the seasons may be responsible for the high char-EC concentrations. However, it is also possible that some of the particles were emitted from motor vehicles, considering the characteristics of sampling site and the relatively high char-EC concentration observed in summer.

Fig. 7 shows the correlations of OC and Char-EC with $NO_x$ and NO concentrations in FPs and UFPs. The bulk of $NO_x$ is emitted by the high temperature combustion of fossil fuels. The main emission source of $NO_x$ at roadside environment would be motor vehicles. $NO_x$ is primarily emitted as NO which oxidizes to $NO_2$. The typical lifetime of $NO_x$ is the order of 4 to 20 h depending on season and the spatial scale of $NO_x$ is an urban or local scale (Seinfeld

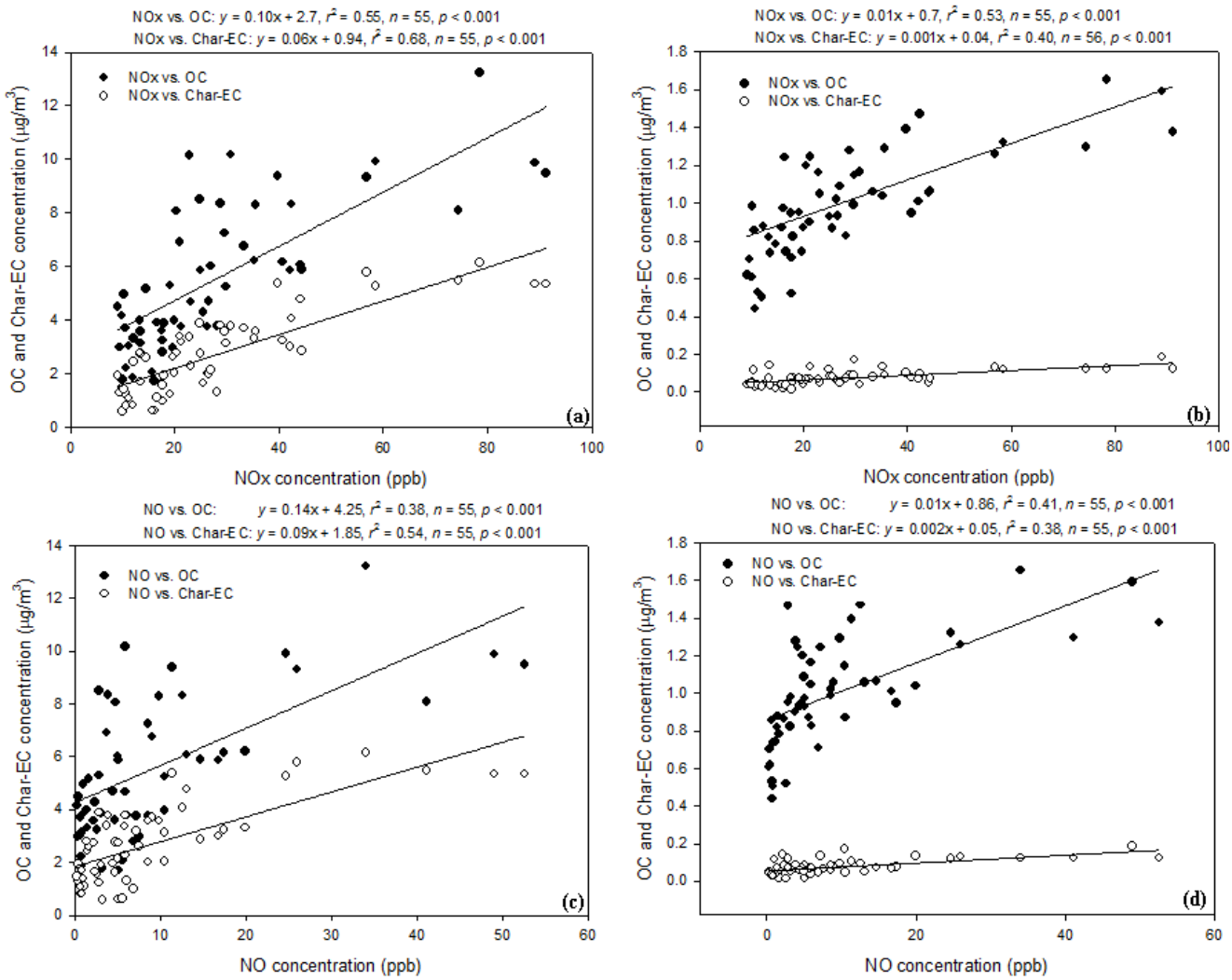


**Fig. 7.** Correlations of OC and char-EC with $NO_x$ and NO concentrations in FPs and UFPs over the four seasons: (a) OC and char-EC versus $NO_x$ in FPs; (b) OC and char-EC versus $NO_x$ in UFPs; (c) OC and char-EC versus NO in FPs; and (d) OC and char-EC versus NO in UFPs.

and Pandis, 2006). More recent study carried out in Los Angeles, USA (Su *et al*., 2009) reported that the reactive pollutants such as NO and $NO_2$ could have high spatial extents of lifetime (e.g., > 5,000 m from expressway). Therefore, the use of NO and $NO_x$ concentration data obtained from meteorological station can be valid. Relatively high correlations of $NO_x$ and NO with char-EC in FPs as well as in UFPs were observed in the sampling periods over the four seasons, indicating that char emission from motor vehicles may be possible. Char may be formed and emitted into the ambient air by motor vehicles as a result of incomplete combustion or unusually low combustion temperatures (partially burned fuel). It can also be thought that motor vehicles with low fuel efficiency could emit char with unburned (or partially burned) fuels and lubricating oils because the observed concentrations of char-EC and OC are highly correlated, even though the samples were taken from ambient air.

Several studies have shown high concentrations of char-EC (EC1-POC) in urban areas (Maykut *et al*., 2003; Louie *et al*., 2005) and along heavily trafficked roads (Cao *et al*., 2006). Zhu *et al.* (2010) also observed high char-EC concentrations in samples collected at a tunnel with heavy traffic. The explained the observation of high char-EC by the catalytic effect of metals on soot oxidation, which would lower the soot oxidation temperature and would cause high-temperature soot to evolve as low-temperature soot in the carbon fraction determination, thus leading to a much higher char-EC fraction than originally contained in the soot. Metal catalysis might be one reason for the observed high char-EC, but this is unlikely to explain their observation fully. There is also a possibility that diesel engines also emit char or char-like particles via incomplete combustion. Filippo and Maricq (2008) observed diesel nucleation mode particles such as semivolatile or solid particles in their diesel particle filter (DPF). They observed that the particles remained nonvolatile at temperatures greater than 400°C and had a bipolar charge with a Boltzmann temperature of 580°C. They concluded that the "solid" nuclei particles form during combustion but remain distinct from soot particles. They might have observed the existence of char particles in their experiment. Furthermore, Moldanova *et al.* (2009) conducted a study on the characterization of particulate matter and gaseous emissions from a large ship diesel engine; they observed the morphology of particles and then identified the existence of char and char-mineral particles from diesel exhaust. Of course, a large ship diesel engine and a typical diesel engine could be different, but their findings show the possibility of char particle emission from a diesel engine.

### *Morphological Characteristics of Collected Particles*

TEM was used to observe morphological characteristics of the collected particles. The samples were chosen on the basis of the observed OC, char-EC, and soot-EC concentrations (1 UFP sample and 2 FP samples). The concentrations of OC, char-EC, and soot-EC in the selected UFP sample were 1.67, 0.12, and 0.08 μg/m$^3$, respectively (Fig. 8(a)). Two FP samples were chosen to observe their differing morphological characteristics. One FP sample represents low soot-EC (0.22 μg/m$^3$) with relatively high OC (9.87 μg/m$^3$) and char-EC (5.35 μg/m$^3$) concentrations (Fig. 8(b) and (e)); the other represents high soot-EC (0.86 μg/m$^3$) with relatively low OC (1.86 μg/m$^3$) and char-EC (0.83 μg/m$^3$) concentrations (Fig. 8(c) and (f)). Char particle could be observed as well (Fig. 8(d)).

Soot agglomerates in UFPs and FPs are shown in Fig. 8(a) and (b), respectively. The shape of soot agglomerates in UFPs and FPs resembles the shape of typical DEPs. The soot agglomerates in UFPs (Fig. 8(a)) consisting of primary particles appear to be coated with condensed materials. The soot agglomerates in FPs (Fig. 8(b)) whose OC concentration is high (9.87 μg/m$^3$) also appear to be coated with condensed materials and consist of larger primary particles (*ca*. 40–70 nm) whereas those in FPs (Fig. 8(c)) whose OC concentration is relatively low (1.86 μg/m$^3$) appear to be smaller, crystallized, and consisted of smaller primary particles (*ca*. 20–40 nm). The shape of the low-OC and high-OC particles differs notably. The primary soot particle size has been reported to vary depending on engine operating conditions, injector type, and injector conditions but most primary particles sizes range from 20 to 70 nm (Bruce *et al*., 1991; Lee *et al*., 2001). These morphological characteristics of soot agglomerates reflect the size of the primary soot particles as well as the OC concentration of the particles collected and observed. These morphological characteristics of collected FPs also support the observed positive and negative correlations between soot-EC and OC in UFPs and FPs, respectively, which were discussed in Section 3.2.4.

Char particles of between approximately 180 and 220 nm also could be observed in the TEM analysis (Fig. 8(d)), although we could not determine whether this char particle originated from biomass burning or motor vehicle combustion. The morphological characteristics of atmospheric particles could also provide us important qualitative information on the collected particle sources and characteristics.

## CONCLUSIONS

Atmospheric carbonaceous components, particularly char and soot in UFPs and FPs, were measured four times during one year (2009–2010) in Saitama City, Japan. In this study, interesting results were obtained by observing the chemical composition of UFPs and FPs, which represent the particles with the highest number and mass concentrations in an urban environment, respectively. It was found that EC accounts for 33–37% of TC in FPs, whereas EC accounts for 12–20% of TC in UFPs over the four seasons. Both char-EC and soot-EC account for similar proportions of the total EC concentration in UFPs, while soot-EC accounts for only a small fraction of the total EC in FPs, indicating that char-EC is mainly composed of large particles and soot-EC is composed of much smaller particles.

The observed positive correlation between OC and soot-EC in UFPs may reflect the compactness (high density) of

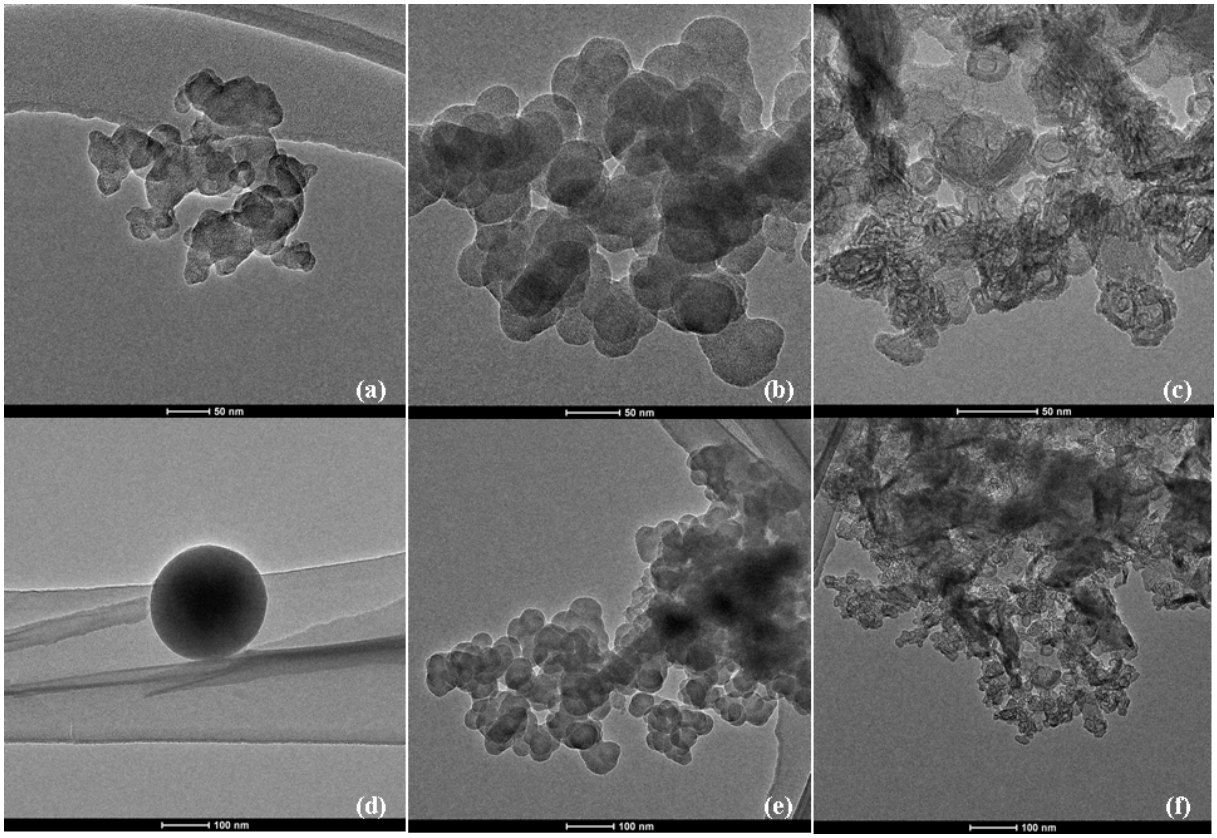


**Fig. 8.** TEM images of soot agglomerates in UFPs and FPs, and char particles in FPs: (a) soot agglomerates in UFPs; (b) soot agglomerates with low soot and high OC concentrations in FPs; (c) soot agglomerates with high soot and low OC concentrations in FPs; (d) char particle; (e) zoomed-out image of (b); and (f) zoomed-out image of (c).

UFPs coated with condensed material such as unburned fuel or lubricating oil. The negative correlation between OC and soot-EC in FPs may also indicate that whether or not the spaces between primary particles in FPs can be filled depends on the engine load of diesel vehicles operated near the sampling site. Thus, the finding indicates that the study area was significantly influenced by motor vehicle emissions. The observed positive and negative correlations were stronger for UFPs ($r^2 = 0.69$, $n = 29$, $p < 0.001$) and FPs ($r^2 = –0.62$, $n = 29$, $p < 0.001$) when the data collected at wind speed greater than 2.5 m/s were excluded. This further confirms the strong influence of motor vehicles at the sampling site. The morphological characteristics of the collected particles, as observed by TEM, also support the relationship between soot-EC and OC. Considering the relatively high char-EC concentration in the roadside environment, even in summer, we conclude that combustion in motor vehicles may produce char or char-like particles. Further study is necessary to confirm this finding.

## ACKNOWLEDGEMENTS

This study was supported in part by a Grant-in-Aid for Scientific Research (Kakenhi, No. 21120502) from the Ministry of Education, Culture, Sports, Science and Technology (MEXT) of Japan.

## REFERENCES

Bond, T.C. (2007). Can Warming Particles Enter Global Climate Discussions? *Environ. Res. Lett.* 2: 045030.

Bond, T.C., Bhardwaj, E., Dong, R., Jogani, R., Jung, S., Roden, C., Streets, D.G., Fernandes, S. and Trautmann, N. (2007). Historical Emissions of Black and Organic Carbon Aerosol from Energy-related Combustion, 1850-2000. *Global Biogeochem. Cycles* 21: GB2018, doi: 10.1029/2006GB002840.

Bruce, C.W., Stromberg, T.F., Gurton, K.P. and Mozer, J.B. (1991). Trans-spectral Absorption and Scattering of Electromagnetic Radiation by Diesel Soot. *Appl. Opt.* 30: 1537–1546.

Cao, J.J., Lee, S.C., Ho, K.F., Fung, K., Chow, J.C. and Watson, J.G. (2006). Characterization of Roadside Fine Particulate Carbon and its Eight Fractions in Hong Kong. *Aerosol Air Qual. Res.* 6: 106–122.

Chameides, W.L. and Bergin, M. (2002). Soot Takes Center Stage. *Science* 297: 2214–2215.

Chow, J.C., Watson, H.G., Chen, L.W.A., Arnott, W.P. and Moosmuller, H. (2004). Equivalence of Elemental Carbon by Thermal/Optical Reflectance and Transmittance with Different Temperature Protocols. *Environ. Sci. Technol.* 38: 4414–4422.

Chow, J.C., Watson, J.G., Pritchett, L.C., Pierson, W.R., Frazier, C.A. and Purcell, R.G. (1993). The DRI

Thermal/Optical Reflectance Carbon Analysis System: Description, Evaluation and Applications in U.S. Air Quality Studies. *Atmos. Environ.* 27: 1185–1201.

Eryu, K., Seto, T., Mizukami, Y., Nagura, M., Furuuchi, M., Tajima, M., Kato, T., Ehara, K. and Otani, Y. (2009). Design of Inertial Filter for Classification of $PM_{0.1}$. *Earozoru Kenkyu* 24: 24–29 (*Written in Japanese*).

Funasak, K., Miyazaki, T., Kawaraya, T., Tsuruho, K. and Mizuno, T. (1998). Characteristics of Particulates and Gaseous Pollutants in Highway Tunnel. *Environ*. *Pollut*. 102: 171–176.

Furuuchi, M., Choosong, T., Hata, M., Otani, Y., Tekasakul, P., Takizawa, M. and Nagura, M. (2010b). Development of a Personal Sampler for Evaluating Exposure to Ultrafine Particles. *Aerosol Air Qual. Res.* 10: 30–37.

Furuuchi, M., Eryu, K., Nagura, M., Hata, M., Kato, T., Tajima, N., Sekiguchi, K., Ehara, K., Seto, T. and Otani, Y. (2010a). Development and Performance Evaluation of Air Sampler with Inertial Filter for Nanoparticle Sampling. *Aerosol Air Qual. Res.* 10: 185–192.

Hagino, H., Takada, T., Kunimi, H. and Sakamoto, K. (2007). Characterization and Source Presumption of Wintertime Submicron Organic Aerosols at Saitama, Japan, Using the Aerodyne Aerosol Mass Spectrometer. *Atmos. Environ.* 41: 8834–8845.

Han, Y.M., Cao, J.J., Chow, J.C., Watson, J.G., An, Z.S., Jin, Z., Fung, K. and Liu, S. (2007). Evaluation of the Thermal/Optical Reflectance Method for Discrimination between Char- and Soot-EC. *Chemosphere* 69: 569–574.

Han, Y.M., Cao, J.J., Lee, S.C., Ho, K.F. and An, Z.S. (2010). Different Characteristics of Char and Soot in the Atmosphere and their Ratio as an Indicator for Source Identification in Xi'an, China. *Atmos. Chem. Phys.* 10: 595–607.

Han, Y.M., Lee, S.C., Cao, J.J., Ho, K.F. and An, Z.S. (2009). Spatial Distribution and Seasonal Variation of Char-EC and Soot-EC in the Atmosphere over China. *Atmos. Environ.* 43: 6066–6073.

Hansen, J. and Nazarenko, L. (2004). Soot Climate Forcing Via Snow and Ice Albedos. *Proc. Nat. Acad. Sci. U.S.A.* 101: 423–428.

Hansen, J., Sato, M., Ruedy, R., Lacis, A. and Oinas, V. (2000). Global Warming in the Twenty-first Century: An Alternative Scenario. *Proc. Nat. Acad. Sci. U.S.A.* 97: 9875–9880.

Haywood, J.M. and Ramaswamy, V. (1998). Global Sensitivity Studies of the Direct Radiative Forcing due to Anthropogenic Sulfate and Black Carbon Aerosols. *J. Geophys. Res.* 103: 6043–6058.

Ho, K.F., Cao, J.J., Harrison, R.M., Lee, S.C. and Bau, K.K. (2004). Indoor/Outdoor Relationships of Organic Carbon (OC) and Elemental Carbon (EC) in $PM_{2.5}$ in Roadside Environment of Hong Kong. *Atmos*. *Environ*. 38, 6327–6335.

Jacobson, M.A. (2001). Strong Radiative heating due to the Mixing State of Black Carbon in Atmospheric Aerosols. *Nature* 409: 695–697.

Jacobson, M.A. (2004). Climate Response of Fossil Fuel and Biofuel Soot Accounting for Soot's Feedback to Snow and Sea Ice Albedo and Emissivity. *J. Geophys. Res.* 109: D21201, doi: 10.1029/2004JD004945.

Jacobson, M.Z. (2006). Effects of Externally-through-internally-mixed Soot Inclusions within Clouds and Precipitation on Global Climate. *J. Geophys. Res.* 110: 6860–6873.

Kittelson, D.B. (1998). Engines and Nanoparticles: A Review. *J. Aerosol Sci.* 29: 574–588.

Kittelson, D.B. (1999). Ultrafine Particulate Matter in the Exhaust from Diesel and Gasoline-powered Mobile Sources. Presented to the Mobile Sources Technical Review Sub-committee, p. 33–34. http://transaq.ce.gatech.edu/epatac/documents/kittelsn.pdf.

Lee, K.O., Cole, R., Sekar, R., Choi, M.Y., Zhu, J., Kang, J. and Bae, C. (2001). Detailed Characterization of Morphology and Dimensions of Diesel Particulates Via Thermophoretic Sampling. *SAE* 2001-01-3572.

Louie, P.K.K., Watson, J.G., Chow, J.C., Chen, A., Sin, D.W.M. and Lau, A.K.H. (2005). Seasonal Characteristics and Regional Transport of $PM_{2.5}$ in Hong Kong. *Atmos. Environ.* 39: 1695–1710.

Masiello, C.A. (2004). New Directions in Black Carbon Organic Geochemistry. *Mar. Chem.* 92: 201–213.

Maykut, N.N., Lewtas, J., Kim, E. and Larson, E.T. (2003). Source Apportionment of $PM_{2.5}$ at an Urban IMPROVE Site in Seattle, Washington. *Environ. Sci. Technol.* 37: 5135–5142.

Mayol-Bracero, O., Gabriel, R., Andreae, M., Kirchstetter, T., Novakov, T., Ogren, J., Sheridan, P. and Streets, D. (2002). Carbonaceous Aerosols over the Indian Ocean during the Indian Ocean Experiment (INDOEX): Chemical Characterization, Optical Properties, and Probable Sources. *J. Geophys Res.* 107: 8030, doi: 10.1029/2000JD000039

Menon, S., Hansen, J., Nazarenko, L. and Luo, Y. (2002). Climate Effects of Black Carbon Aerosols in China and India. *Science* 297: 2250–2253.

Moldanova, J., Fridell, E., Popvicheva, O., Denmirdjian, B., Tishkova, V., Faccinetto, A. and Focsa, C. (2009). Characterization of Particulate Matter and Gaseous Emissions from a Large Ship Diesel Engine. *Atmos. Environ.* 43: 2632–2641.

Morawska, L., Ristovski, Z., Jayaratne, E.R., Keogh, D.U. and Ling, X. (2008). Ambient Nano and Ultrafine Particles from Motor Vehicle Emissions: Characteristics Ambient Processing and Implications on Human Exposure. *Atmos. Environ.* 42: 8113–8138.

Otani, Y., Eryu, K., Furuuchi, M., Tajima, N. and Tekasakul, P. (2007). Inertial Classification of Nanoparticles with Fibrous Filters. *Aerosol Air Qual. Res.* 7: 343–352.

Park, K., Cao, F., Kittelson, D.B. and McMurry, P.H. (2003). Relationship between Particle Mass and Mobility for Diesel Exhaust Particles. *Environ. Sci. Technol.* 37: 577–583.

Ramanathan, V. and Carmichael, G. (2008). Global and Regional Climate Changes due to Black Carbon. *Nat. Geosci.* 1: 221–227.

Ramanathan, V., Crutzen, P.J., Kiehl, J.T., Rosenfeld, D. (2001). Atmosphere: Aerosols, Climate, and the

Hydrological cycle. *Science* 294: 2119–2124.

Ramanathan, V., Li, F., Ramana, M.V., Praveen, P.S., Kim, D., Corrigan, C.E., Nguyen, H., Stone, E.A., Schauer, J.J., Carmichael, G.R., Adhikary, B. and Yoon, S.C. (2007). Atmospheric Brown Clouds: Hemispherical and Regional Variations in Long-range Transport, Absorption, and Radiative Forcing. *J. Geophys. Res.* 112: D22S21, doi: 10.1029/2006JD008124.

Schichtel, B.A., Malm, W.C., Bench, G., Fallon, S., McDade, C.E., Chow, J.C. and Watson, J.G. (2008). Fossil and Contemporary Fine Particulate Carbon Fractions at 12 Rural and Urban Sites in the United States. *J. Geophys. Res.* 113: D02311, doi: 10.1029/2007JD008605.

Seinfeld, J.H. and Pandis, S.N. (2006). *Atmospheric Chemistry and Physics: From Air Pollution to Climate Change*, 2nd Edition, John Wiley Sons, Inc, New Jersey.

Su, J.G., Jerrett, M., Beckerman, B., Wilhelm, M., Ghosh, J.K. and Ritz, B. (2009). Predicting Traffic-related Air Pollution in Los Angeles Using a Distance Decay Regression Selection Strategy. *Environ. Res.* 109: 657–670.

Symonds, J.P.R., Reavell, K.St.J., Olfert, J.O., Campbell, B.W. and Swift, S.J. (2007). Diesel Soot Mass Calculation in Real-time with a Differential Mobility Spectrometer. *J. Aerosol Sci.* 38: 52–68.

USAID (2010). USAID Report on *Black Carbon Emissions in Asia*, United States Agency for International Development.

Veilleux, M.H., Dickens, A.F., Brandes, J. and Gelinas, Y. (2009). Density Separation of Combustion-derived Soot and Petrogenic Graphitic Black Carbon: Quantification and Isotopic Characterization. *Earth Environ. Sci.* 5: 1–9.

Zhu, C.S., Chen, C.C., Cao, J.J., Tsai, C.J., Chou Charles, C.K., Liu, S.C. and Roam, G.D. (2010). Characterization of Carbon Fractions for Atmospheric Fine Particles and Nanoparticles in a Highway Tunnel. *Atmos. Environ.* 44: 2668–2673.

*Received for review, July 27, 2010*
*Accepted, October 17, 2010*